*Published online 5 February 2010*

*Nucleic Acids Research, 2010, Vol. 38, No. 9* ***e108***
*doi:10.1093/nar/gkq049*

# Dual FRET assay for detecting receptor protein interaction with DNA

**Tomasz Krusiński, Andrzej Ożyhar and Piotr Dobryszycki***

Wroclaw University of Technology, Faculty of Chemistry, Division of Biochemistry, Wybrzeże Wyspiańskiego 27, 50-370 Wrocław, Poland

Received March 9, 2009; Revised January 15, 2010; Accepted January 18, 2010

## ABSTRACT

**We present here a new assay that is based on the idea of the molecular beacon. This assay makes it possible to investigate two proteins interacting with DNA at two binding sites that are close to each other. The effectiveness of the test depends on the exclusive binding of three DNA fragments in the presence of two proteins, and the monitoring of the process depends upon observing the quenching of two independent fluorescence donors. As a model we used the components of the heterodimeric ecdysteroid receptor proteins ultraspiracle (Usp) and ecdysone receptor (EcR) from *Drosophila melanogaster* and a response element from the promoter of the *hsp27* gene. The response element consists of two binding sites (half-sites) for the DNA binding domains (DBDs). We have shown that protein–protein interactions mediate cooperative binding of the ecdysteroid receptor DBDs to a $hsp27_{pal}$ response element. The analysis of the microscopic dissociation constants obtained with the DMB led to the conclusion that there was increased affinity of UspDBD to the 5′ half-site in the presence of EcRDBD when the 3′ half-site was occupied, and increased affinity of EcRDBD to the 3′ half-site when the 5′ half-site was occupied.**

## INTRODUCTION

Proteins which bind to DNA often form oligomeric complexes. Such complexes have been observed for a lot of nuclear receptors which function as homo- or heterodimeric proteins, e.g. homodimeric steroid hormone receptors (GR, MR, PR, AR, ER), orphan homodimeric receptors (RXR, COUP-TF, HNF-4, revErb) and heterodimers with RXR (RAR, TR, VDR, LXR, NGFI-B, EcR) as well as yeast transcription factors such as MATa1 and MATα2, a complex required for the repression of mating type genes in a cell type-specific manner (1–6). Functional ecdysteroid receptor, which was used as a model for the present studies, consists of two proteins: EcR and ultraspiracle (Usp), products of the *EcR* and *Usp* genes (7,8). Usp is a homolog of the human RXR protein (9). The EcR/Usp heterodimer regulates transcription in insects through a $hsp27_{pal}$ natural 20-hydroxyecdysone response element (HRE), which is an imperfect palindrome from the promoter region of the *Drosophila melanogaster hsp27* gene (10). Previous analysis of EcR/Usp interaction showed that UspDBD acts as a specific anchor that preferentially binds the 5′ half-site of the $hsp27_{pal}$ ($hsp27_{pal\text{-}5'}$), and thus places the EcR/Usp complex in the defined orientation (10-14). Moreover, we used FRET technology to study the UspDBD/EcRDBD-$hsp27_{pal}$ complex topology. Fluorescence data indicated that UspDBD determines the architecture of the heterocomplex UspDBD/EcRDBD which is caused by significant deformation (DNA bending) of the response element, whereas EcRDBD plays the role of a specific helper molecule (15). Neither protein forms a complex in solution in the absence of the response element.

The study of protein–DNA interactions is currently one of the fastest developing fields of molecular biology. Some of the techniques can be used to identify DNA binding proteins, giving direct information on the molecular basis of the interaction—the location of the DNA binding site, the strength and specificity of binding or of protein binding on gross conformation and the local structure of DNA. Quantification of the level of activity of specific proteins is one of the most commonly performed experiments in biomedical research. Determination of the DNA binding affinities can be done by, e.g. the filter binding assay, SPR measurements, steady-state fluorescence measurements and sometimes under appropriate conditions the electrophoretic mobility shift assay (EMSA). EMSA can often allow the resolution of multiple species of DNA–protein complexes, but the most important limitation is the lack of equilibrium during electrophoresis (16). The purpose of our work was to propose an analytical method which would help us to precisely define the

*To whom correspondence should be addressed. Tel: +48 71 320 6340; Fax: +48 71 320 6337; Email: piotr.dobryszycki@pwr.wroc.pl

affinity of the two-protein receptor to DNA and the interaction mechanism of both proteins with each other. The respective dissociation constants (but not the cooperativity factors) were compared to the fluorescence anisotropy data, and the results obtained with the help of molecular beacons with a single FRET donor–acceptor pair (17,18). We believe that in the future it would be possible to use a similar system in biosensors. EMSA measurements were done as a qualitative control of the newly formed protein–DNA complexes.

Using molecular beacons (MB) for DNA binding proteins is a recently developed technology (19,20) that attempts to overcome the limitations of antibody usage or the necessity of applying expensive methods like, for example, surface plasmon resonance (21,22). MBs have historically been used as hairpin-shaped oligonucleotide probes that report the presence of a specific target sequence. When bound to their targets MBs undergo a conformational reorganization that restores the fluorescence of an internally quenched fluorophore. MBs are usually oligonucleotide probes that can indicate the presence of particular nucleic acids in solution (23,24). Interestingly, molecular beacon assemblies can also detect sequence-specific DNA binding proteins (17,25–28). This type of test depends on binding exclusively in the presence of protein, two DNA fragments, which together form the protein binding site. We have also recently demonstrated a solid-phase immobilized MB designated for protein–DNA interaction studies. The system was successfully applied to detect the sequence-specific interaction of a natural response element from the promoter of the *hsp27* gene with the DNA binding domains of ecdysteroid receptor proteins (18).

The sensitivity of the typical stem and loop test was improved and described previously. The enhanced test used a four-component system of complementary oligonucleotides with double fluorescence resonance energy transfer (FRET) (29). It was based on the idea of binding three ss 9-mers to the target ss 27-mer labeled with three fluorescence probes (one donor and two acceptors) to form a fully assembled dsDNA. A single base mismatch could be detected with the described double FRET system. Similar MBs with two FRET-pairs were described previously (30–33). They usually consisted of two ordinary MBs whose fluorophores formed one donor–acceptor pair. Both MBs used sequences complementary to adjacent regions on the same oligonucleotide target such that FRET occurred only when both beacons were hybridized to the target (33). The system was successfully used for mRNA detection in living cells and for monitoring changes of mRNA level and mRNA cell localization (34).

In this article, we present the dual FRET assay (DMB) for the independent quantitative analysis of the binding affinity of dimerizing DNA binding proteins with two specific DNA sites in proximity to each other. We have developed a new approach using a 64-bp fragment of $hsp27_{pal}$ labeled with two donor– quencher pairs. The DNA sequences were designed to hybridize with complementary fragments only in the presence of the protein molecule(s), and they were chosen in such a way that the protein binding sequences were divided into three parts (Left, Middle and Right) and two of them (Left and Middle or Middle and Right) were necessary for binding each protein (Figure 1A). Reconstitution of the regulatory sequence brought each of the FRET-pairs into proximity and led to fluorescence signal quenching as a result of the resonance energy transfer between the donors and the quencher probes. Since the design of the described assay is not limited to any specific protein, it would be possible to develop a DMB for a variety of target proteins which recognize specific DNA sequences. Quantification of the microscopic dissociation constants (Figure 1B) of both ecdysteroid receptor forming protein DBDs showed that the binding clearly displays a cooperative character.

## MATERIALS AND METHODS

### Double FRET molecular beacon preparation

The following oligonucleotides were used for DMB preparation: 5′-TGAGGAGCAGCACGAAGCGAGA C-3′ (O1), FL-5′-AAGGGTTCAATGCACTTG-3′-Cy5.5 (O2), 5′-TCCAATGAAAATACAAGCTCTGT-3′ (O3), 5′-ACAGAGCTTGTATTTTCAT**B**GGACAAGTGC AT-3′ (O4), 5′-TGAACCCTTG**D**CTCGCTTCGTGCTG CTCCTCA-3′ (O5), where: **D,** dT-dabcyl (dT-DAB) and **B**; dT-BHQ-3, fluorescence quenchers; FL, fluorescein; and Cy5.5, fluorescence donors.

Setting up a DMB requires three independent fragments (L, M, R) (Figure 1A). We prepared two annealed fragments of respective sequences of O1–O5 (L) and O3–O4 (R). M corresponds to the ssDNA O2 sequence. A 9-bp overhang from the L duplex was complementary to the 5′ half of the M sequence, labeled with the nonfluorescent energy quencher dabcyl. The R duplex contained a 9-bp overhang complementary to the 3′ half of the M and labeled with the nonfluorescent energy quencher BHQ-3. Both O1–O5 and O3–O4 oligonucleotide pairs of 10 μM concentration were mixed in a 50 mM Tris buffer (100 mM NaCl, 5 μM $ZnCl_2$, 1 mM DTT, pH 7.8 at 25°C) heated to 96°C for 1 min and then cooled to room temperature for 2.5 h to obtain DNA duplexes. Hybridization of L, M and R caused the reconstruction of the full-length DNA duplex (64 bp; shortened in Figure 1A) containing the $hsp27_{pal}$ response element sequence (10). Oligonucleotide concentrations were calculated from the absorption spectra of oligonucleotide solutions recorded from 200 to 750 nm using 236 300 $M^{-1}cm^{-1}$ (O1), 176 700 $M^{-1}cm^{-1}$ (O2), 227 900 $M^{-1}cm^{-1}$ (O3), 313 300 $M^{-1}cm^{-1}$ (O4) and 273 800 $M^{-1}cm^{-1}$ (O5) extinction coefficients (according to the manufacturer, IBA, Germany; Biomers.net; Germany). Absorption spectra were recorded with a Cary 300 UV-VIS (Varian Inc., USA) and Ultrospec 4000 UV/VIS (Pharmacia Biotech, USA) spectrophotometers. All measurements were performed in a 50 mM Tris buffer (100 mM NaCl, 5 μM $ZnCl_2$, 1 mM DTT, pH 7.8 at 25°C) at 25°C.

In order to interpret the fluorescence data, the emission spectrum of the oligonucleotide labeled with one donor (FL) should be separated from the absorption (excitation) spectrum of the second donor (Cy5.5) to limit the FRET

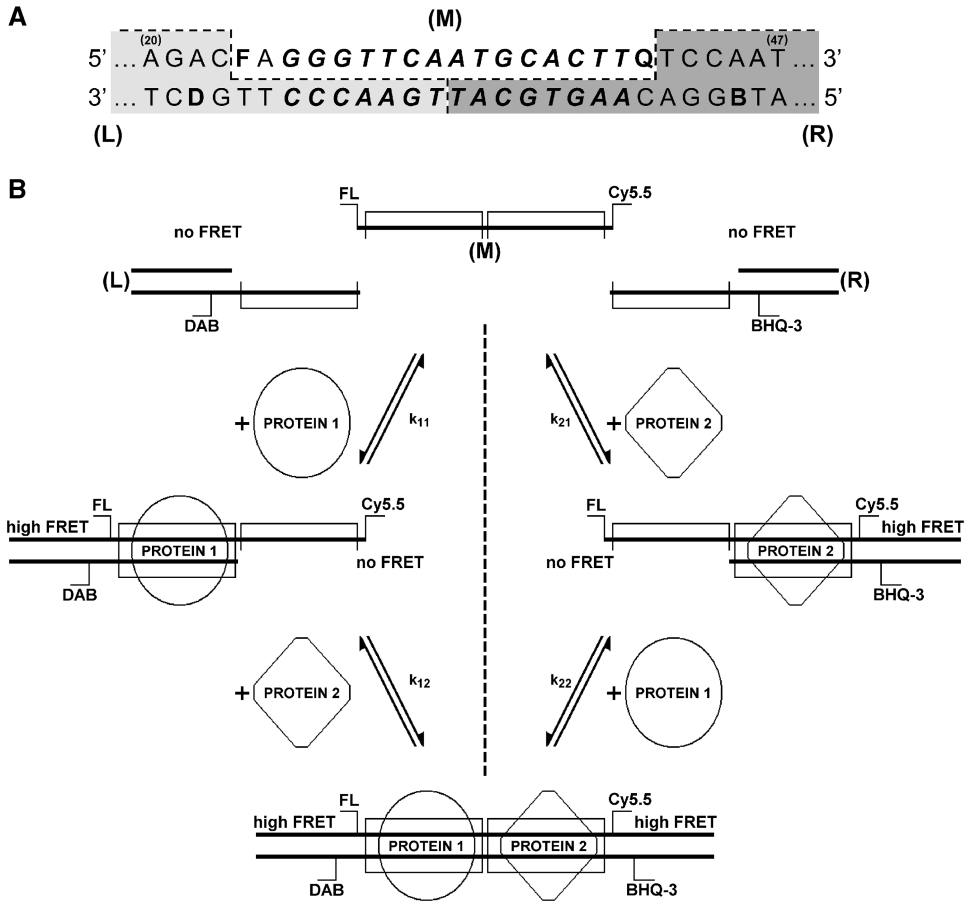


**Figure 1.** The scheme of the dual FRET assay consisting of the regulatory element $hsp27_{pal}$ and showing the model of interaction with the UspDBD and EcRDBD proteins. (**A**) The broken line separates the parts of the DMB. M denotes middle ss-DNA, L the left duplex and R the right duplex; the UspDBD and/or EcRDBD binding-site is marked with italic bold letters; fluorophore and quencher labels: F denotes FL-5′-A, Q is Cy5.5-3′-G, D is dT-DAB, and B is dT-BHQ-3. The numbers in parentheses correspond to the bp numbers of the full length DMB used. (**B**) The overall design of the DMB assay for determining the dimeric DNA binding protein affinity to the DNA response element with microscopic dissociation constants ($k_{nn}$). The association of two-donor-labeled middle (M) ss-DNA fragments and two quencher-labeled DNA half-sites (with a 9 bp overhang) in the presence of two proteins (PROTEIN 1 and PROTEIN 2). FL (fluorescein) means fluorescence donor, DAB (dabcyl) is the fluorescence quencher, Cy5.5 is the fluorescence donor, BHQ-3 is the fluorescence quencher, L the left DNA duplex and R the right DNA duplex. High FRET was observed when FL was in close proximity to DAB, and when Cy5.5 was close to BHQ-3.

between them. The spectra of the dyes which was used exhibited a small, negligent overlap between the FL emission spectrum and Cy5.5 absorption spectrum (Supplementary Figure S1).

### Protein preparation

The expression and purification of the UspDBD and the EcRDBD proteins was performed as previously described (13). To improve the final purity of the proteins, one additional step was added to the procedure. In particular, DBD that contained fractions from the glutathione-Sepharose 4B (Amersham Biosciences, Freiburg, Germany) column were applied to a heparin-Sepharose CL-6B (Amersham Biosciences) column equilibrated with a 20 mM Tris buffer (150 mM NaCl, 1 mM DTT, 5 μM $ZnCl_2$, pH 7.8 at 25°C). Fractions of 1.0 ml were eluted at a flow rate of 0.25 ml/min with 10 ml of an equilibration buffer and then with 10 ml of the same buffer containing 400 mM NaCl. The DBD was eluted with 10 ml of the equilibration buffer containing 650 mM NaCl, concentrated with an Amicon Ultra-4 centrifugal filter device (Millipore, USA) to about 0.2 ml, and applied onto a Superdex 75 HR (Amersham Biosciences) column operated as described previously (35). The DBDs were found to be at least 98% homogeneous when analyzed by SDS–PAGE densitometry (not shown). The concentrations of the protein samples were determined using the following absorption coefficients: 7000 $M^{-1}cm^{-1}$ (UspDBDs); 5840 $M^{-1}cm^{-1}$ (EcRDBD) (35).

### EMSA procedure

EMSAs (35) were performed using the Protean II electrophoresis system (Bio-Rad, USA). Briefly, the indicated amounts of protein(s) and 60 pmol of the appropriate oligonucleotide(s) were incubated for 30 min on ice

in a final volume of 25 ml in a 50 mM Tris buffer (100 mM NaCl, 5 μM $ZnCl_2$, 1 mM DTT, pH 7.8 at 25°C). The receptor–DNA complexes were separated from the free DNA in a 12% nondenaturing polyacrylamide gel ($20 \times 16 \times 0.15$ cm) run in a $0.25 \times$ TBE buffer (22.25 mM Tris, 22.25 mM borate, 0.5 mM EDTA, pH 8.3 at 25°C) immediately after incubation. The experiment was performed at 25°C and 4°C. The gel was prerun at 160 V for 90 min. After applying the samples the electrophoresis was continued for 480 min at 270 V. Gels were stained with Stains-All dye (Sigma-Aldrich, USA) using the protocol described previously (37,38).

### Fluorescence measurements

The spectra of oligonucleotides labeled with the fluorescence probes were recorded with the Fluorolog-3-21 fluorometer (Spex, Jobin Yvon Inc., France) in 115F-QS quartz cells (Hellma, Germany) using an excitation wavelength of $\lambda_{EX-1} = 497$ nm for the FL-modified oligonucleotide and $\lambda_{EX-2} = 675$ nm for Cy5.5. Titration experiments were done with a Microlab 500 automatic titrator (Hamilton, USA) in a 101F-QS quartz cell (Hellma, Germany). The changes in the fluorescence intensity of the DNA titrated with proteins were corrected for the dilution effect and the decrease in the time-dependent fluorescence signal of the fluorophore-labeled oligonucleotides. The control measurements were done in the same manner as described above, except the solution of unlabeled oligonucleotide or Tris buffer replaced the labeled oligonucleotide or protein solution, respectively. All measurements were performed in a 50 mM Tris buffer (100 mM NaCl, 5 μM $ZnCl_2$, 1 mM DTT, pH 7.8 at 25°C) at 25°C.

### Estimation of the dissociation constants

The two-step experiment consisted of equilibrium titrations of the middle DNA fragment (M) which was doubly labeled with fluorescence donors (FL and Cy5.5). The left (L) and right (R) DNA duplexes were labeled with the quencher dyes dabcyl (DAB) and BHQ-3, respectively, and titrations of all three (L, M and R) DMB fragments were done with UspDBD and/or EcRDBD protein. Data from the first step were analyzed by the nonlinear regression fitting according to Equations (1) and (2):

$$F_{518} = f_{11} \cdot [M] + f_{21} \cdot [L:M] \quad (1)$$

$$F_{691} = f_{12} \cdot [M] + f_{22} \cdot [M:R] \quad (2)$$

where: $F_\lambda$ is the fluorescence intensity observed at λ wavelength; $f_{11}$ and $f_{12}$ are the specific fluorescence intensity of M at 518 and 691 nm respectively; $f_{21}$ and $f_{22}$ are the specific fluorescence intensity of duplexes containing L and M fragments ($L$:$M$) or M and R fragments ($M$:$R$), respectively; $[M]$ is the equilibrium concentration of the M; $[L$:$M]$ and $[M$:$R]$ are the equilibrium concentration of L:M and M:R duplexes, respectively. Data points were analyzed according to Equations (3) and (4):

$$F_{518} = F_{MAX} + (F_{MIN} - F_{MAX}) \times \frac{\left((K_{1-5'} + [M]_T + [L]_T) - \sqrt{(K_{1-5'} + [M]_T + [L]_T)^2 - 4 \cdot [M]_T \cdot [L]_T}\right)}{2 \cdot [M]_T} \quad (3)$$

$$F_{691} = F_{MAX} + (F_{MIN} - F_{MAX}) \times \frac{\left((K_{1-3'} + [M]_T + [R]_T) - \sqrt{(K_{1-3'} + [M]_T + [R]_T)^2 - 4 \cdot [M]_T \cdot [R]_T}\right)}{2 \cdot [M]_T} \quad (4)$$

where $F$ is the observed fluorescence intensity; $F_{MAX}$ is the maximal value of the fluorescence intensity; $F_{MIN}$ is the fitted value of the minimal fluorescence intensity, $K_{1-5'}$ is the dissociation constant of the L:M complex; $K_{1-3'}$ is the dissociation constant of the M:R complex; $[M]_T$, $[L]_T$, $[R]_T$ are the total concentrations of M, L and R, respectively. During the second step of the experiment, the equilibrium titration of all three fragments (L, M and R) of the protein was performed and monitored at 518 nm and 691 nm. Experimental points were fitted to Equations (5) and (6):

$$F_{518} = F_{MAX} + (F_{MIN} - F_{MAX}) \times \frac{\left((K_{app-5'} + [M]_T + [P]_T) - \sqrt{(K_{app-5'} + [M]_T + [P]_T)^2 - 4 \cdot [M]_T \cdot [P]_T}\right)}{2 \cdot [M]_T} \quad (5)$$

$$F_{691} = F_{MAX} + (F_{MIN} - F_{MAX}) \times \frac{\left((K_{app-3'} + [M]_T + [P]_T) - \sqrt{(K_{app-3'} + [M]_T + [P]_T)^2 - 4 \cdot [M]_T \cdot [P]_T}\right)}{2 \cdot [M]_T} \quad (6)$$

where, $K_{app-5'}$ is the apparent dissociation constant of the 5′ binding site-protein complex, $K_{app\text{-}3'}$ is the apparent dissociation constant of the 3′ binding site-protein complex, $[P]_T$ is the total protein concentration. Taking into account the scheme (Figure 1B) of the protein (P) interaction with the 5′($L$:$M$) or 3′ binding site ($M$:$R$) and the calculated values of $K_1$ and $K_{app}$, one can obtain the $K_d$ constant according to Equations (7) and (8), respectively (25,27):

$$K_{d-5'} = \left(\frac{K_{app-5'}}{K_{1-5'}}\right) \cdot [L] \quad (7)$$

$$K_{d-3'} = \left(\frac{K_{app-3'}}{K_{1-3'}}\right) \cdot [R] \quad (8)$$

The final determination of the protein–DNA microscopic $k_{nn}$ values is based on the simple model presented in Figure 1B. The assay involves equilibria between full-length DNA (DNA) and protein molecules (DNA-P5′ and DNA-P3′) described by the microscopic equilibrium constants $k_{11}$ and $k_{12}$. Furthermore, the next equilibria between the DNA-P5′ or DNA-P3′ complex with the second protein molecule, both forming the dimeric protein–DNA complex (DNA-P5′-P3′) described by constants $k_{21}$ and $k_{22}$. $k_{11}$ and $k_{12}$ were determined in independent experiments in which the L–M duplex containing the left binding half-site and the M–R duplex containing the right binding-site, respectively, were titrated with UspDBD, UspDBDΔA or EcRDBD proteins. UspDBDΔA has a truncated A-box, and it binds $hsp27_{pal}$ with an affinity similar to a wild-type protein (39). Concentrations of specific types of DNA were calculated according to the scheme presented in Figure 1B and the following equations:

$$k_{11} = \frac{[\mathrm{DNA}][P]}{[\mathrm{DNA} - P5']} \quad (9)$$

$$k_{12} = \frac{[\mathrm{DNA}][p]}{[\mathrm{DNA} - P3']} \quad (10)$$

$k_{22}$ and $k_{21}$ constant values were obtained from $K_{d-5'}$ and $K_{d-3'}$ as described above for the unsplit regulatory element (L–M–R), assuming:

$$k_{21} = \frac{K_{d-3'}}{k_{12}} = \frac{\sqrt{K_{d-5'} \cdot K_{d-3'}}}{k_{11}} \quad (11)$$

$$k_{22} = \frac{K_{d-5'}}{k_{11}} = \frac{\sqrt{K_{d-5'} \cdot K_{d-3'}}}{k_{12}} \quad (12)$$

All numeric calculations were performed with the help of the nonlinear regression procedure of Levenberg–Marquardt with Origin 7.5 software (OriginLab. Co., USA).

## RESULTS

The molecular beacon-like assay proposed in this article contains two independent FRET pairs comprised of left (L) and right (R) oligonucleotide duplexes labeled with DAB and BHQ-3 quenchers, respectively, and a middle ss-oligonucleotide (M) labeled with donor dyes FL at the 5′-end and Cy5.5 at the 3′-end (Figure 1A). Hybridization of the three components creates the full-length regulatory element (15 bp) plus flanking sequences. The fluorescence emission spectrum of the doubly labeled M when excited at 497 nm has an emission maximum of 518 nm and when excited at 675 nm has a maximum of 691 nm. Separating the DAB and BHQ-3 absorption spectra led to the specific and effective quenching of FL by DAB and Cy5.5 by BHQ-3 (Supplementary Figure S1).

The key for successful dual FRET assay application is the proper choice of fluorophore labels and their position in the DNA sequence. If FL and Cy5.5 are chosen as a pair, there is sufficient separation of the emission and absorption spectra (Supplementary Figure 1S). The donor/quencher pairs FL/ DAB and Cy5.5/BHQ3 also fulfilled the conditions needed for distinct fluorescence quenching. In control experiments, we used oligonucleotides with different positions of fluorescence dyes. The DAB was placed at the 22 position of the full-length 64-bp sequence, FL at the 24 position, Cy5.5 at the 41 position and BHQ-3 at the 45 position (numbering according to Figure 1A). This was the most effective placement and we continued to use these positions in further experiments. When the donor (FL-24) and quencher (DAB-23) probes were too close, quenching of the donor dye was blocked (Figure 2, full circles) probably due to sterically blocked DNA association, while the second donor (Cy5.5-41) was effectively quenched by (BHQ-3-42) (Figure 2, open squares). When there was too long of a distance between the labels (FL-24, DAB-20), the fluorescence quenching considerably decreased (not shown).

Further electrophoretic control experiments were done in order to confirm the accuracy of the model presented in Figure 1B by identifying the protein–DNA species formed. Splitting the regulatory element into three fragments (L, R and M) eliminated protein binding in the absence of the middle M fragment. An EMSA assay indicated that UspDBD or EcRDBD bound to the L or R duplex in the presence of the M oligonucleotide as a monomeric protein–DNA complex (Figure 3, lanes 3, 8 and Supplementary Figure 2S, lanes 3, 4, 8, 9). The dimeric complex was created only in the presence of the full set of L, R, and M fragments (Figure 3, lanes 14, 17, 18, Supplementary Figure 2S, lanes 13–18). UspDBD and/or EcRDBD binding to different DNA fragments could be observed by the decreased intensity of the L/R band at the 4–6, 9–11, 12–14 and 15–18 lanes concomitant with increased protein concentration. For example, in lane 3

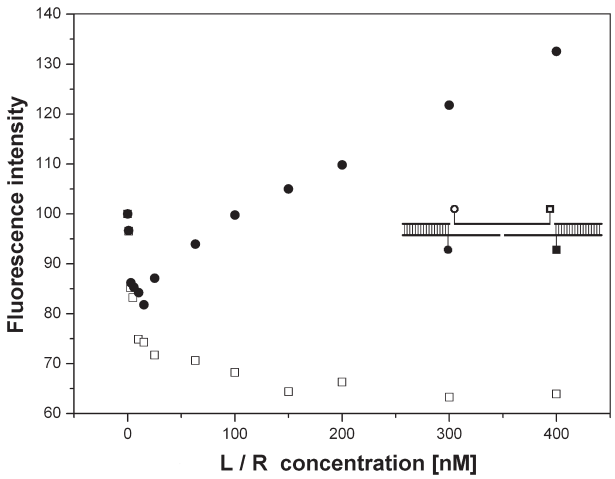


**Figure 2.** The noneffective placement of the donor–quencher pair, FL at the position 24 of the sequence of the regulatory element (numbering according to Figure 1A); DAB at the position 23, respectively, (filled circles). Second fluorophore Cy5.5 at the position 41 is quenched by BHQ-3 -42 (open squares). Titration of the M fragment (10 nM) labeled with fluorescein ($\lambda_{EX}$ = 497 nm, $\lambda_{EM}$ = 518 nm) and Cy5.5 ($\lambda_{EX}$ = 675 nm, $\lambda_{EM}$ = 691 nm) with equimolar amounts of the L and R duplex (L/R) in the absence of protein monitored at 518 nm (filled circles) and 691 nm (open squares).

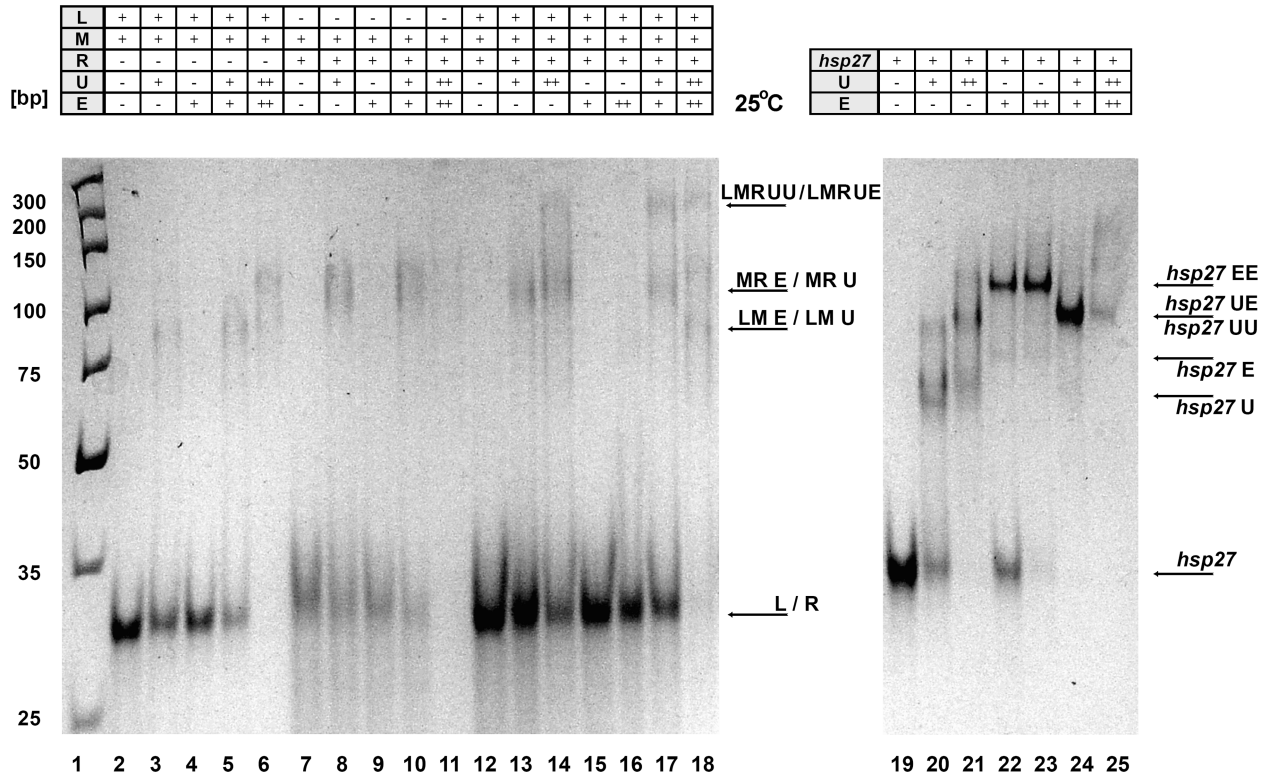


**Figure 3.** Electrophoretic mobility shift titration at 25°C on a 12% nondenaturing polyacrylamide gel of DMB fragments with UspDBD (U) and/or EcRDBD (E) (left panel). EMSA titration of the control 32-bp dsDNA containing an intact ecdysteroid receptor binding site with UspDBD and/or EcRDBD (right panel). '+' denotes 60 pmol (2.4 μM concentration), '++' denotes 120pmol (4.8 μM concentration). Gels were stained with Stains-All dye as described in 'Materials and Methods' section. Lane 1, molecular mass standards; L denotes the left DNA duplex; R the right DNA duplex and M the middle ssDNA; U denotes UspDBD; E is EcRDBD; UU is UspDBD dimer; EE is EcRDBD dimer; and L/R is the left and/or right DNA duplex. Samples were incubated for 30 min before loading on to the gel.

one can see the protein–DNA complex (LMU) and the lower intensity of the band (L) in comparison with lane 2. In lane 4, there was decreased intensity only in the band of unbound DNA (L), and the LME complex was visible only at 4°C (Supplementary Figure S2). In lane 5, most of the unbound DNA (L) was titrated and the complexes LMU and LME are visible. EMSA experiments qualitively illustrated the weaker interaction of EcRDBD in comparison with UspDBD with fragments of the regulatory element. In lane 6, the unbound DNA (L) was almost totally titrated. Results similar to the L DNA duplex were obtained for the R duplex (lanes 7–11). Only at 4°C in lanes 10 and 11 one can see trace amounts of dimeric complexes (MRUE), even though the left binding half-site was absent, probably due to protein–protein interaction that forced nonspecific protein–DNA binding at high protein concentrations (Supplementary Figure S2). The presence of L, R and M fragments induces higher molecular weight species with UspDBD and/or EcRDB such as LMRUU (lanes 13 and 14), LMREE only at 4°C (Supplementary Figure S2, lanes 15 and 16) and LMRUE (lanes 17 and 18). In lanes 7–10 and 12–17, the MR and LM bands were visible only at a low temperature (4°C), which was needed to improve the quality of the EMSA experiments (Supplementary Figure 2S). The result of the control experiment shown in the right panel of Figure 3 is in agreement with the data obtained previously (35). An increasing amount of UspDBD and/or EcRDBD added to the wild-type regulatory element $hsp27_{pal}$ (32 bp) resulted in the formation of monomeric (*hsp27*U, *hsp27*E) and dimeric (*hsp27*UU, *hsp27*EE, *hsp27*UE) protein–DNA complexes. Barely visible bands in the left panel are probably a result of the low amount of corresponding complexes which were formed as a result of the different equilibria of the LM, RM, LMR DNA fragments. The fluorescence quenching of the FL or Cy5.5 fluorophores, both labeled the M fragment, resulted probably from the protein-induced annealing of the two oligonucleotides. No interaction of the UspDBD and/or EcRDBD proteins with the single DMB fragments (L, M or R) was observed in the EMSA experiments. Fluorescence spectra in Figure 4 were normalized to 100% (primary data were in c.p.s.). Protein titration curves (Figure 4A–F) obtained in the protein absence begin at higher c.p.s. values than in the presence of the protein (not shown). Titration of M oligo with L, R or equimolar amounts of L and R (L/R) indicated that regulatory element binding half-sites were stepwise reconstituted in the absence of the protein(s) with the titrant concentration increase. Titration of the oligonucleotide L and M or M and R or L and M and R indicated initial fluorescence quenching in the absence of the protein relative to the fluorescence of M fragment, similarly as in the case of M titration with the remaining

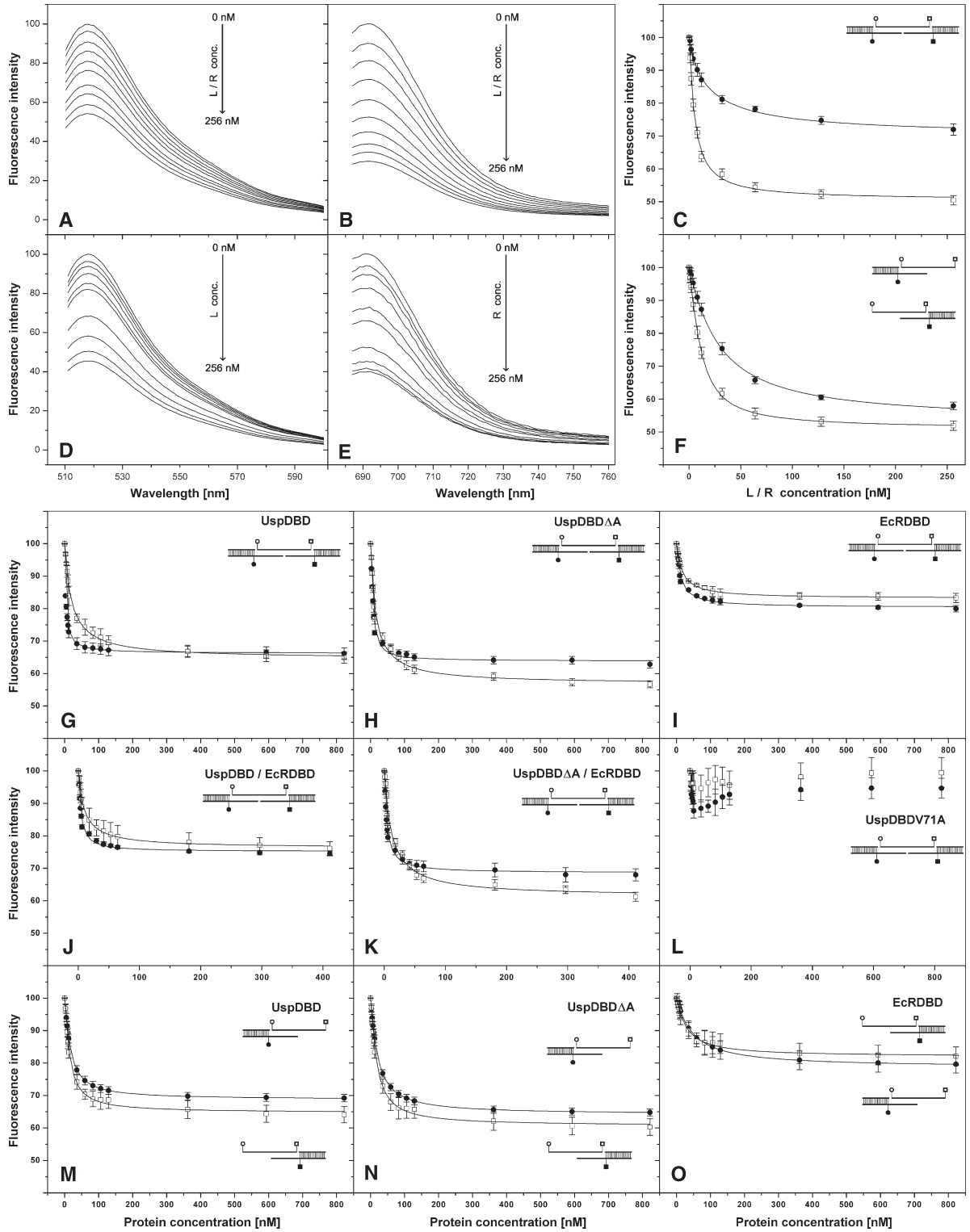


**Figure 4.** Fluorescence quenching of the M fragment (10 nM) labeled with two donors in the absence of protein (**A–F**) and in the presence of protein (**G–O**). Titration of M with increasing amounts (0, 1, 2, 4, 8, 12, 32, 64, 128, 256 nM) of the equimolar mixture of L and R duplexes (L/R) (A–C) or one L or R duplex (D–F). The titration curves of fragment M (10 nM) and two DNA duplexes L (12.5 nM) and R (12.5 nM) labeled with quencher dyes (G–L) and L and M or R and M (M–O) with the UspDBD or EcRDBD proteins (0, 2.4, 4.8, 7.2, 9.6, 12.0, 35.8, 59.4, 82.8, 106, 129, 362, 593, 822 nM) or equimolar mixture of EcRDBD and UspDBD (0, 1.2, 2.4, 3.6, 4.8, 6.0, 17.9, 29.7, 41.4, 53.0, 64.5, 181, 296.5, 411 nM). Emission was monitored after FL excitation with $\lambda_1 = 494$ nm (A and D, filled squares in C, F and G–O) or after excitation of Cy5.5 with $\lambda_2 = 675$ nm (B and E, empty circles in C, F and G–O). The solid line represents the best fit of the data to the model shown in Figure 1B. The diagrams on the right side of the C, F, G–O panels indicate the DMB variants titrated with the protein indicated above. Measurements were performed in a 50 mM Tris buffer (100 mM NaCl, 5 μM $ZnCl_2$, 1 mM DTT, pH 7.8 at 25°C) at 25°C. The DNA fragments were incubated for 30 min before measure and additionally for 5 min after each protein portion was added. Error bars indicate standard deviation values of three measurements. The changes in fluorescence intensity of the titrated DNA probes presented in panels C, F–O, were corrected for the dilution effect and the decrease in the time-dependent fluorescence signal of the fluorophore-labeled oligonucleotides. The uncorrected spectra are shown in (A, B, D and E).

**Table 1.** Macroscopic dissociation constants for the complex of ecdysteroid receptor fragments with the regulatory element $hsp27_{pal}$

| Complex of $hsp27_{pal}$ with | $K_{d-5'}$ (nM) | ± | $K_{d-3'}$ (nM) | ± |
|---|---|---|---|---|
| UspDBD | 0.57 | 0.06 | 6.01 | 0.86 |
| UspDBDΔA | 0.79 | 0.11 | 8.54 | 0.97 |
| UspDBDV71A | Not detected | | Not detected | |
| EcRDBD | 1.99 | 0.15 | 9.49 | 0.63 |
| UspDBD–EcRDBD | 0.54 | 0.08 | 2.54 | 0.54 |
| UspDBDΔA– EcRDBD | 1.04 | 0.11 | 9.84 | 1.13 |

**Table 2.** Microscopic dissociation constants and cooperativity factors for the complexes of ecdysteroid receptor fragments with the regulatory element $hsp27_{pal}$

| Complex of $hsp27_{pal}$ with | $k_{11}$ (nM) | ± | $k_{21}$ (nM) | ± | $\omega_{21}$[a] | ± |
|---|---|---|---|---|---|---|
| UspDBD | 1.23 | 0.09 | 1.52 | 0.21 | 2.74 | 0.63 |
| UspDBDΔA | 1.72 | 0.12 | 1.53 | 0.21 | 3.39 | 0.76 |
| EcRDBD | 4.08 | 0.36 | 1.08 | 0.12 | 8.52 | 2.00 |
| UspDBD – EcRDBD | 1.23 | 0.09 | 0.97 | 0.17 | 9.74 | 2.88 |
| UspDBDΔA–EcRDBD | 1.72 | 0.12 | 1.75 | 0.22 | 5.29 | 1.32 |
| Complex of $hsp27_{pal}$ with | $k_{12}$ (nM) | ± | $k_{22}$ (nM) | ± | $\omega_{22}$[a] | ± |
| UspDBD | 4.03 | 0.38 | 0.47 | 0.07 | 2.71 | 0.59 |
| UspDBDΔA | 5.03 | 0.45 | 0.53 | 0.08 | 3.36 | 0.73 |
| EcRDBD | 8.96 | 1.14 | 0.50 | 0.07 | 8.43 | 1.90 |
| UspDBD–EcRDBD | 8.96 | 1.14 | 0.27 | 0.13 | 6.14 | 3.29 |
| UspDBDΔA–EcRDBD | 8.96 | 1.14 | 0.37 | 0.06 | 4.83 | 1.11 |

[a]$\omega_{21} = k_{12}/k_{21}$ and $\omega_{22} = k_{11}/k_{22}$.

oligos. It indicates the existence of a small fraction of the reconstituted 5′and/or 3′ half-sites. Taking into account the assumption that UspDBD and EcRDBD preferentially bind 5′ and 3′ regulatory element half-sites, respectively (13) one can conclude that the proteins bind to the respective half-sites, shift the equilibrium and promote reconstruction of the full length *hsp27* (more complexes of LM and MR occupied with the protein excess).

In the first step of the quantitative analysis using the DMB assay, titration of the donor-labeled central element (M) (Figure 1A) was performed with a large excess of L labeled with two quenchers and/or R duplexes in the absence of the protein. The association between the two DNA half-sites caused recovery of a single binding site even in the absence of the protein and made it possible to calculate the $K_{1\text{-}5'}$ and $K_{1\text{-}3'}$ dissociation constants (see Equations 3–8). Ten nanomolars of the fragment M treated with 0–256 nM each of the DAB-labeled L 5′ half-site and the BHQ-3-labeled R half-site decreased the fluorescence intensities monitored at 518 or 691 nm by about 28% and 50%, respectively (Figure 4A and B). The titration curves and the good fit of the data points to the model described by Equations (3) and (4) are shown in Figure 4A–F. The calculated values of $K_{1\text{-}5'}$ and $K_{1\text{-}3'}$ were 23.70 ± 1.55 nM and 6.17 ± 0.27 nM, respectively.

The second step of the analysis was based on the titration of a mixture of the DMB fragments with UspDBD and EcRDBD. The titration curves and the fit of the data points to the model described by Equations (5) and (6) are shown in Figure 4G–L. The values for $K_{app\text{-}5'}$ and $K_{app\text{-}3'}$ obtained in the presence of EcRDBD were 18.75 ± 0.19 and 23.35 ± 0.54 nM, respectively. The dissociation constants of the protein–DNA complexes ($K_{d-3'}$ and $K_{d-5'}$) were calculated with Equations (7) and (8) using $K_{app-5'}$ and $K_{1-5'}$ or $K_{app-3'}$ and $K_{1-3,}$ respectively (Table 1). Also, the $K_{app-5'}$ and $K_{app-3'}$ values were obtained in the presence of UspDBD and consequently the $K_{d-5'}$ for UspDBD–$hsp27_{pal\text{-}5'}$ and $K_{d-3'}$ for UspDBD–$hsp27_{pal-3'}$ complex formation.

In the last step of the analysis, using Equations (9–12), we determined the microscopic dissociation constants $k_{11}$, $k_{12}$, $k_{21}$, $k_{22}$ and the cooperativity factors, $\omega$, describing the association of the full-length (L–M–R) $hsp27_{pal}$ element with DNA binding proteins, i.e. the association of a monomeric protein in the absence ($k_{11}$, $k_{12}$) or presence ($k_{21}$, $k_{22}$) of a partner (Figure 1B, Table 2). The experiment was performed by titrating a solution containing L, M or M, R DNA fragments (Figure 1A) with UspDBD or EcRDBD (Figure 4M–O). The excellent fit of the experimental data shown in Figure 4 indicate that the model illustrated in Figure 1 B is sufficient to describe the DMB assay in the presence of dimeric protein.

Analysis of the dissociation constants obtained with the DMB showed new properties of the ecdysteroid receptor. UspDBD has higher affinity to both the 5′ and 3′ half-sites than EcRDBD in the absence of the second half-site ($k_{11}$, $k_{22}$). The biggest change in affinity to the 3′ half-site was induced by EcRDBD when the 5′ half-site was occupied ($k_{21}$ against $k_{12}$). UspDBD in the presence of EcRDBD showed a higher affinity to the 5′ half-site when the 3′ half-site was occupied (compare $k_{22}$ with $k_{11}$). EcRDBD showed a higher affinity to the 3′ half-site when the 5′ half-site was occupied ($k_{21}$ with $k_{12}$). EcRDBD formed a homodimeric complex on the $hsp27_{pal}$ element with greater affinity than UspDBD ($k_{21}$ for both proteins) when the 5′ half-site was occupied. UspDBDΔA caused a negative effect on the heterodimerization with EcRDBD in comparison with the wild-type protein ($k_{21}$ and $k_{22}$ of the heterodimer formation).

To examine DMB sensitivity and the ability to distinguish between mutant proteins with different activities, we decided to use variants of UspDBD, i.e. UspDBDΔA, as a positive control and nonbonding UspDBDV71A as a negative control. Single-point mutated UspDBD protein with Ala at position 71 instead of Val was previously shown to be essential for preserving the native protein structure and a significantly lower affinity to $hsp27_{pal}$ (17,18,40).

## DISCUSSION

The process of protein heterodimerization facilitates receptor binding to the HRE, increases the specificity of complex formation and enables the differentiation of the HRE from target sequences for homodimeric receptors (41). It is also essential for binding repressor complexes (42). Most nuclear receptors dimerize by cooperatively binding their DBDs to the regulatory elements. Moreover, dimerization of DBDs is strictly dependent

on the defined regulatory element characteristic for each protein–DNA complex, and therefore is not observed in solution in the absence of DNA (43,44). There is a serious analytical problem in determining the role of the individual elements which build receptor complexes. In some cases it is possible to practice EMSA measurements, which unequivocally identify protein–DNA complexes (36). However, quantitative analysis of this assay is limited because of disadvantageous experimental conditions that are far from being in equilibrium. Dissociation constants obtained in this way can differ about two orders of magnitude in comparison with the values obtained with equilibrium methods like various spectroscopic methods (45). In addition, differences in the EMSA results obtained at 4°C and 25°C (Figure 3 and Supplementary Figure 2S), probably stem from the relatively low stability of EcRDBD protein at 25°C in relation to UspDBD (46).

It is also possible to more easily determine dissociation constants and the bonding stoichiometry of simple 1:1 protein DNA complexes using the fluorescence anisotropy methodology (47). A serious disadvantage of the widely used fluorescence anisotropy measurements is that they are not sufficiently sensitive, because of small changes in the anisotropy signal during the formation of a protein–DNA complex (48–51). The problem of calculating the dissociation constants ($K_d$) grows with the complexity of the examined set of molecules.

The new DMB technology presented in this paper provides sensitive detection of heterodimeric protein activity in a way that could be easily applied to determine dissociation constants. The protein detection is done using inexpensive, easily synthesized oligonucleotides, accompanied by a fluorescence readout. An important point is that detecting the two targeted proteins and reporting the signal occur simultaneously and independently, increasing the potential for using this technology in high throughput analysis. DMB methodology was successfully applied to the detection and quantitative analysis of the sequence-specific interaction of a natural $hsp27_{pal}$ response element with UspDBD and EcRDBD in a way that could be readily applied to real-time imaging or to biosensors. Our results are consistent with those obtained by conventional fluorescence titrations and by FRET measurements with molecular beacons (17, 18) and confirmed the earlier published results of EMSA experiments, which showed that dimer 5′UspDBD-3′EcRDBD is formed in a preferential way on the regulatory element and that the UspDBDΔA mutant demonstrates a slightly lower affinity to the regulatory element than the wild-type protein (13). Equilibrium data presented in this article demonstrates the validity of the model presented in Figure 1B and indicates the usefulness of the assay, which may be applied as a standard MB for biosensor preparation and for quantitative analysis of the interaction of dimeric receptors with a target regulatory sequence. The analysis of the microscopic dissociation constants obtained with the DMB led to interesting conclusions that show new properties of the receptor and the role of an individual protein in the formation of an active complex. For example, there was increased affinity to the regulatory element induced by EcRDBD when the 5′ half-site was occupied, increased affinity of UspDBD in the presence of EcRDBD to the 5′ half-site when the 3′ half-site was occupied and increased affinity of EcRDBD to the 3′ half-site when the 5′ half-site was occupied. This cooperative effect is described by the respective constants ($\omega$), which show that protein–DNA interactions are strongly influenced by protein–protein interactions (Table 2).

It was previously shown with EMSA experiments that protein–protein interactions also mediate cooperative binding of the glucocorticoid receptor DBD, a member of a family of transcription factors (52,53). The authors showed that binding to a low affinity half-site is dependent on the previous occupancy of the high affinity half-site. However, the calculation of the extent of the cooperation was based on a nonequilibrium assay and the assumption of two identical binding sites, which may not be valid. Our technique is free of such assumptions and shows the anisotropy of the formation of the protein–DNA complex and the cross-talk effect of the EcRDBD protein with UspDBD (Table 2). The highest values of the $\omega$-factor were observed for the formation of the heterodimeric complex EcRDBD–UspDBD-$hsp27_{pal}$ in comparison with homodimeric complexes and complexes with UspDBDΔA. Our data allowed us to precisely distinguish between the HRE half-sites.

## SUPPLEMENTARY DATA

Supplementary Data are available at NAR Online.

## ACKNOWLEDGEMENTS

We thank our colleague Michał Jakób for assistance in developing the procedures for obtaining the UspDBD and EcRDBD proteins for this study.

## FUNDING

Wroclaw University of Technology. Funding for open access charge: Polish Ministry of Science and Higher Education (grant number 3552/P01/2006/31).

*Conflict of interest statement*. None declared.

## REFERENCES

1. Claessens,F. and Gewirth,D.T. (2004) DNA recognition by nuclear receptors. *Essays Biochem.*, **40**, 59–72.
2. Escriva,H., Bertrand,S. and Laudet,V. (2004) The evolution of the nuclear receptor superfamily. *Essays Biochem.*, **40**, 11–26.
3. Gronemayer,H. and Miturski,R. (2000) Molecular Mechanism of Retinoid Action. *Cell Mol. Biol. Lett.*, **6**, 3–52.
4. Phillips,C.L., Stark,M.R., Johnson,A.D. and Dahlquist,F. (1994) Heterodimerization of the yeast homeodomain transcriptional regulators α2 and a1 induces an interfacial helix in α2. *Biochemistry*, **33**, 9294–9302.
5. Tan,S., Hunziker,Y., Pellegrini,L. and Richmond,T.J. (2000) Crystallization of the yeast MATα2/MCM1/DNA ternary complex: general methods and principles for protein/DNA cocrystallization. *J. Mol. Biol.*, **297**, 947–959.
6. King-Jones,K. and Thummel,C.S. (2005) Nuclear receptors - a perspective from Drosophila. *Nat. Rev. Genet.*, **6**, 311–323.

7. Koelle,M.R., Talbot,W.S., Segraves,W.A., Bender,M.T., Cherbas,P. and Hogness,D.S. (1991) The Drosophila EcR gene encodes an ecdysone receptor, a new member of the steroid receptor superfamily. *Cell*, **67**, 59–77.
8. Oro,A.E., McKeown,M. and Evans,R.M. (1990) Relationship between the product of the Drosophila ultraspiracle locus and the vertebrate retinoid X receptor. *Nature*, **347**, 298–301.
9. Oro,A.E., McKeown,M. and Evans,R.M. (1992) The Drosophila retinoid X receptor homolog ultraspiracle functions in both female reproduction and eye morphogenesis. *Development*, **115**, 449–462.
10. Riddihough,G. and Pelham,H.R. (1987) An ecdysone response element in the Drosophila hsp27 promoter. *EMBO J.*, **6**, 3729–3734.
11. Martinez,E., Givel,F. and Wahli,W. (1991) A common ancestor DNA motif for invertebrate and vertebrate hormone response elements. *EMBO J.*, **10**, 263–268.
12. Ożyhar,A., Strangmann-Diekmann,M., Kiltz,H.H. and Pongs,O. (1991) Characterization of a specific ecdysteroid receptor-DNA complex reveals common properties for invertebrate and vertebrate hormone-receptor/DNA interactions. *Eur. J. Biochem.*, **200**, 329–335.
13. Niedziela-Majka,A., Kochman,M. and Ozyhar,A. (2000) Polarity of the ecdysone receptor complex interaction with the palindromic response element from the hsp27 gene promoter. *Eur. J. Biochem.*, **267**, 507–519.
14. Jakób,M., Kołodziejczyk,R., Orłowski,M., Krzywda,S., Kowalska,A., Dutko-Gwóźdź,J., Gwóźdź,T., Kochman,M., Jaskólski,M. and Ożyhar,A. (2007) Novel DNA-binding element within the C-terminal extension of the nuclear receptor DNA-binding domain. *Nucleic Acids Res.*, **35**, 2705–2718.
15. Dobryszycki,P., Grad,I., Krusiński,T., Michaluk,P., Sawicka,D., Kowalska,A., Orłowski,M., Jakób,M., Rymarczyk,G., Kochman,M. *et al.* (2006) The DNA-binding domain of the ultraspiracle driver deformation of the response element whereas the DNA-binding domain of the ecdysone receptor is responsible for a slight additional change of the preformed structure. *Biochemistry*, **45**, 668–675.
16. Hellman,L.M. and Fried,M.G. (2007) Electrophoretic shift assay (EMSA) for detecting protein-nucleic acid interactions. *Nat. Protocol*, **2**, 1849–1861.
17. Krusiński,T., Wietrzych,M., Grad,I., Ożyhar,A. and Dobryszycki,P. (2008) Equilibrium analysis of the DNA binding domain of the ultraspiracle protein interaction with the response element from the *hsp27* gene promoter—the application of molecular beacon technology. *J Fluoresc.*, **18**, 1–10.
18. Krusiński,T., Laskowska,A., Ożyhar,A. and Dobryszycki,P. (2008) The application of an immobilized molecular beacon for the analysis of the DNA binding domains from ecdysteroid receptor proteins Usp and EcR's interaction with the *hsp27* response element. *J. Biomol. Screen.*, **13**, 899–905.
19. Li,J.J., Fang,X., Schuster,S.M. and Tan,W. (2000) Molecular beacons: a novel approach to detect protein-DNA interactions. *Angew Chem. Int. Ed. Engl.*, **39**, 1049–1052.
20. Fang,X., Li,J.J. and Tan,W. (2000) Using molecular beacons to probe molecular interactions between lactate dehydrogenase and single-stranded DNA. *Anal. Chem.*, **72**, 3280–3285.
21. Jost,J.P., Munch,O. and Andersson,T. (1991) Study of protein-DNA interactions by surface plasmon resonance (real time kinetics). *Nucleic Acids Res.*, **19**, 2788.
22. Peixoto,P., Liu,Y., Depauw,S., Hildebrand,M.-P., Boykin,D.W., Bailly,C., Wilson,W.D. and David-Cordonnier,M.-H. (2008) Direct inhibition of the DNA-binding activity of POU transcription factors Pit-1 and Brn-3 by selective binding of a phenyl-furan-benzimidazole dication. *Nucleic Acids Res.*, **36**, 3341–3353.
23. Tyagi,S. and Kramer,F.R. (1996) Molecular beacons: probes that fluoresce upon hybridization. *Nat. Biotechnol.*, **14**, 303–308.
24. Tyagi,S., Bratu,D.P. and Kramer,F.R. (1998) Multicolor molecular beacons for allele discrimination. *Nat. Biotechnol.*, **16**, 49–53.
25. Heyduk,T. and Heyduk,E. (2002) Molecular beacons for detecting DNA binding proteins. *Nat. Biotechnol.*, **20**, 171–176.
26. Heyduk,E., Knoll,E. and Heyduk,T. (2003) Molecular beacons for detecting DNA binding proteins: mechanism of action. *Anal. Biochem.*, **316**, 1–10.
27. Knoll,E. and Heyduk,T. (2004) Unimolecular beacons for the detection of DNA-binding proteins. *Anal. Chem.*, **76**, 1156–1164.
28. Dummit,B. and Chang,Y.-H. (2006) Molecular beacons for DNA binding proteins: an emerging technology for detection of DNA binding proteins and their ligands. *Assay Drug Dev. Technol.*, **4**, 343–349.
29. Horsey,I., Furey,W.S., Harrison,J.G., Osborne,M.A. and Balasubramanian,S. (2000) Double fluorescence resonance energy transfer to explore multicomponent binding interactions: a case study of DNA mismatches. *Chem. Commun.*, 1043–1044.
30. Li,J.J., Geyer,R. and Tan,W. (2000) Using molecular beacons as a sensitive Fluorescence assay for enzymatic cleavage of single-stranded DNA. *Nucleic Acids Res.*, **28**, e52.
31. Molenaar,C., Marras,S.A., Slats,J.C.M., Truffert,J.-C., Lemaître,M., Raap,A.K., Dirks,R.W. and Tanke,H.J. (2001) Linear 2' O-Methyl RNA probes for the visualization of RNA in living cells. *Nucleic Acids Res.*, **29**, e89.
32. Tsourkas,A., Behlke,M.A., Xu,Y. and Bao,G. (2003) Spectroscopic features of dual fluorescence/luminescence resonance energy-transfer molecular beacons. *Anal. Chem.*, **75**, 3697–3703.
33. Santangelo,J.P., Nix,B., Tsourkas,A. and Bao,G. (2004) Dual FRET molecular beacons for mRNA detection in living cells. *Nucleic Acids Res.*, **32**, e57.
34. Rhee,W.J., Santangelo,P.J., Jo,H. and Bao,G. (2008) Target accessibility and signal specificity in live-cell detection of BMP-4 mRNA using molecular beacons. *Nucleic Acids Res.*, **36**, e30.
35. Niedziela-Majka,A., Rymarczyk,G., Kochman,M. and Ozyhar,A. (1998) GST-Induced dimerization of DNA-binding domains alters characteristics of their interaction with DNA. *Protein Expr. Purif.*, **14**, 208–220.
36. Fried,M. and Crothers,D.M. (1981) Equilibria and kinetics of lac repressor-operator interactions by polyacrylamide gel electrophoresis. *Nucleic Acids Res.*, **9**, 6505–6525.
37. Campbell,K.P., MacLennan,D.H. and Jorgensen,A.O. (1983) Staining of the $Ca^{2+}$-binding proteins, calsequestrin, calmodulin, troponin C, and S-100, with the cationic carbocyanine dye "Stains-All". *J. Biol. Chem.*, **258**, 11267–11273.
38. Goldberg,H.A. and Warner,K.J. (1997) The staining of acidic proteins on polyacrylamide gels: Enhanced sensitivity and stability of "stains-all" staining in combination with silver nitrate. *Anal. Biochem.*, **251**, 227–233.
39. Grad,I., Niedziela-Majka,A., Kochman,M. and Ożyhar,A. (2001) Analysis of Usp DNA binding domain targeting reveals critical determinants of the ecdysone receptor complex interaction with the response element. *Eur. J. Biochem.*, **268**, 3751–3758.
40. Kowalska,A., Rymarczyk,G., Grad,I., Orłowski,M., Krowarsch,D. and Ożyhar,A. (2003) Residues of the C-terminal region (T-box) of the Ultraspiracle nuclear receptor DNA binding domain crucial to specific interaction with the *hsp27* response element. *Acta Biochim. Pol.*, **50**, 99.
41. Glass,C.K. (1994) Differential recognition of target genes by nuclear receptor monomers, dimers, and heterodimers. *Endocr. Rev.*, **15**, 391–407.
42. Zamir,I., Dawson,J., Lavinsky,R.M., Glass,C.K., Rosenfeld,M.G. and Lazar,M.A. (1997) Cloning and characterization of a corepressor and potential component of the nuclear hormone receptor repression complex. *Proc. Natl Acad. Sci. USA*, **94**, 14400–14405.
43. Mader,S., Chen,J.Y., Chen,Z., White,J., Chambon,P. and Gronemeyer,H. (1993) The patterns of binding of RAR, RXR and TR homo- and heterodimers to direct repeats are dictated by the binding specificities of the DNA binding domains. *EMBO J.*, **12**, 5029–5041.
44. Perlmann,T., Rangarajan,P.N., Umesono,K. and Evans,R.M. (1993) Determinants for selective RAR and TR recognition of direct repeat HREs. *Genes Dev.*, **7**, 1411–1422.
45. Fahrer,J., Kranaster,R., Altmeyer,M., Marx,A. and Bürkle,A. (2007) Quantitative analysis of the binding affinity of poly(ADP-ribose) to specific binding proteins as a function of chain length. *Nucleic Acids Res.*, **35**, e143.

46. Orłowski,M., Szyszka,M., Kowalska,A., Grad,I., Zoglowek,A., Rymarczyk,G., Dobryszycki,P., Krowarsch,D., Rastinejad,F., Kochman,M. *et al.* (2004) Plasticity of the ecdysone receptor DNA binding domain. *Mol. Endocrinol.*, **18**, 2166–2184.
47. Crichlow,G.V., Zhou,H., Hsiao,H., Frederick,K.B., Debrosse,M., Yang,Y., Folta-Stogniew,E.J., Chung,H.-J., Fan,C., De La Cruz,E.M. *et al.* (2008) Dimerization of FIR upon FUSE DNA binding suggests a mechanism of *c*-myc inhibition. *EMBO J.*, **27**, 277–289.
48. LeTilly,V. and Royer,A.C. (1993) Fluorescence anisotropy assays implicate protein-protein interactions in regulating trp repressor DNA binding. *Biochemistry*, **32**, 7753–7758.
49. Boyer,M., Poujol,N., Margeat,E. and Royer,C.A. (2000) Quantitative characterization of the interaction between purified human estrogen receptor α and using fluorescence anisotropy. *Nucleic Acids Res.*, **28**, 2494–2502.
50. Szatkowski-Ozers,M., Hill,J.J., Ervin,K., Wood,J.R., Nardulli,A.M., Royer,C.A. and Gorski,J. (1997) Equilibrium binding of estrogen receptor with DNA using fluorescence anisotropy. *J. Biol. Chem.*, **272**, 30405–30411.
51. Zhao,Q., Chasse,S.A., Sierk,S.D.M.L., Ahvazi,B. and Rastinjad,F. (2000) Structural basis of RXR-DNA interactions. *J. Mol. Biol.*, **296**, 509–520.
52. Dahlman-Wright,K., Wright,A., Diltala-Roos,H., Carlstedt-Duke,J. and Gustafsson,J.-A. (1990) Protein-protein interactions facilitate DNA binding by the glucocorticoid receptor DNA-binding domain. *J. Biol. Chem.*, **265**, 14030–14035.
53. Dahlman-Wright,K., Wright,A., Gustafsson,J.-A. and Carlstedt-Duke,J. (1991) Interactions of the glucocorticoid receptor DNA-binding domain with DNA as a dimer is mediated by a short segment of five amino acids. *J. Biol. Chem.*, **266**, 3107–3112.